

Combining Local and Global Perception for Autonomous Navigation on Nano-UAVs

Lorenzo Lamberti¹, Georg Rutishauser², Francesco Conti¹, and Luca Benini^{1,2}

¹ DEI, University of Bologna, Italy,

² Integrated Systems Laboratory, ETH Zürich, Switzerland.

Abstract. A critical challenge in deploying unmanned aerial vehicles (UAVs) for autonomous tasks is their ability to navigate in an unknown environment. This paper introduces a novel vision-depth fusion approach for autonomous navigation on nano-UAVs. We combine the visual-based PULP-Dronet [1] convolutional neural network for semantic information extraction, i.e., serving as the *global perception*, with 8×8 px depth maps for close-proximity maneuvers, i.e., the *local perception*. When tested in-field, our integration strategy highlights the complementary strengths of both visual and depth sensory information. We achieve a 100% success rate over 15 flights in a complex navigation scenario, encompassing straight pathways, static obstacle avoidance, and 90° turns.

1 Introduction

With their sub-10 cm diameter and tens of grams in weight, autonomous nano-sized unmanned aerial vehicles (UAVs) hold the potential to be employed in a wide range of applications, from inspection of hazardous environments [2] to warehouses [3]. Their small size enables access to confined spaces [1,4], and safe operation near humans [3,5], making them suitable for indoor environments.

Autonomous navigation is a pivotal requirement for any UAV exploring an environment while avoiding obstacles. State-of-the-Art (SoA) navigation systems typically combine global and local planning techniques that are computationally heavy, relegating their execution to high-end devices such as GPUs [6]. On the one hand, global planning is in charge of setting high-level destination goals, for example, ensuring the UAV is passing through pre-defined checkpoints. On the other hand, local planning handles close proximity maneuvers, like obstacle avoidance, ensuring progress toward the goals set by the global planner.

The miniaturized form factor of nano-drones imposes significant constraints on their onboard computing devices, ultimately relying on low-power Micro-Controller Units (MCUs) with a power envelope of ~ 100 mW [1]. Consequently, SoA navigation algorithms on autonomous nano-UAV rely on computationally affordable solutions rather than complex planning strategies. The exploration policies deployed by [7,8] have to rely on basic state machines and single-beam VL53L1x Time-of-Flight (ToF) sensors for collision avoidance. However, the limited field of view (FoV) (15°) of this ToF sensor challenges the detection of narrow obstacles [9]. Müller *et al.* [4] developed a depth-based navigation system for nano-UAVs, utilizing a novel multizone ToF sensor and implementing a lightweight decision tree based on 8×8 px depth maps. While ToF sensors offer

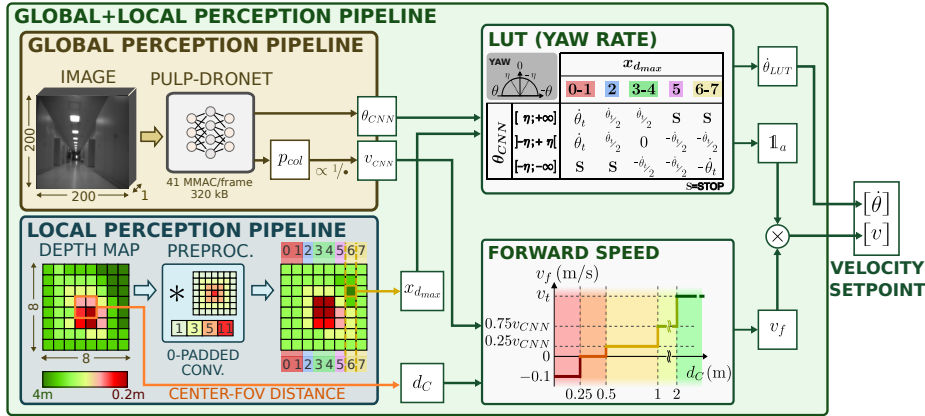


Fig. 1: Our global + local perception pipeline.

geometrically precise measurements of three-dimensional objects in the environment, they lack semantic information. Visual-based navigation approaches, such as the SoA PULP-Dronet [1] convolutional neural network (CNN), are better equipped to process semantically rich non-volumetric visual cues, such as lanes on a floor, that are invisible to ToF sensors. On the other hand, these methods do not extract any precise geometric information about objects in the FoV, posing challenges for obstacle avoidance. While some research has explored the synergy between vision and depth sensors on nano-drones [5,9], their focus has not been on autonomous navigation applications.

In this work, we take one step towards bringing the global and local planning paradigm aboard nano-UAVs. We present a pipeline for autonomous navigation on nano-drones that integrates both *global* and *local* perception. The *global perception* pipeline utilizes the PULP-Dronet CNN for semantic information extraction, while the *local perception* outputs close-proximity (~ 4 m) obstacle-free navigation area. We fuse the visual-depth information with a lightweight lookup table approach, which maps all possible combinations of outputs from the local and global perception pipelines to drone control commands.

Our fused perception pipeline achieved a 100% success rate on a set of fifteen flights, successfully navigating through straight pathways, executing 90° turns, and avoiding static obstacles. In the same scenario, using only the global perception pipeline led to failures in static obstacle avoidance. Conversely, when relying solely on the local perception pipeline, the system failed to handle 90° turns due to the absence of semantic features in the input data. Our results highlight the benefit of combining depth and vision sensory inputs to enhance nano-UAV navigation while also revealing the limitations of depending solely on one sensor type in complex navigation scenarios.

2 System design

Robotic platform. We use the Bitcraze Crazyflie 2.1, a 27-gram, 10-cm diameter nano-drone. The onboard STM32 MCU processor manages sensor interfacing

and low-level flight control tasks. We extend the platform with three printed circuit boards (PCBs). The *AI-deck* serves as the visual navigation engine, featuring a GWT GAP8 9-core RISC-V-based System-on-Chip (SoC) and a grayscale QVGA Himax HM01B0 camera with a 115° FoV. In the GAP8 architecture, a single core handles system operations, including UART communication with the STM32 MCU, while the general-purpose 8-core cluster is used for CNN processing. We use the open-source *Multizone Ranger Deck* [4], featuring a front-looking VL53LC5CX1 matrix ToF sensor. This sensor, connected to the STM32 over the I2C bus, acquires 8×8 px depth maps with a 65° FoV at a frequency of 15 Hz and with a range of 0.2–4 m. Last, the *Flow deck v2*, a downward-facing PCB that provides the STM32 MCU with height measurements from the ground and horizontal motion estimation based on optical flow.

Global + local perception pipelines. Our autonomous navigation pipeline for nano-UAVs, depicted in Figure 1, comprises several components, all executed onboard. The *global perception pipeline* is constituted by the PULP-Dronet [1], a CNN for visual-based navigation on nano-UAVs. We use the pre-trained weights of [1]. The CNN takes 200×200 px images as input and produces two outputs: a steering angle θ_{CNN} and a collision probability p_{col} . This CNN runs on the 8-core cluster of the GAP8 SoC at 19 FPS. As in [1], we post-process the PULP-Dronet outputs, computing the forward speed v_{CNN} inversely proportional to p_{col} , while the steering angle θ_{CNN} is rescaled into a yaw-rate.

The *local perception pipeline* executes entirely on the STM32 MCU. We acquire the 8×8 px depth map from the front-looking matrix ToF sensor. Then, we convolve the depth map with a 2-D Gaussian kernel, requiring only 1600 MAC operations, to identify the most free area within the input. The input is zero-padded to maintain consistent input-output dimensions and to favor navigation toward the center of the ToF FoV when no obstacles are present. Finally, we determine the x-coordinate ($x_{d_{max}}$) of the pixel with the longest distance in the 8×8 depth map. This coordinate ranges from 0 to 7, denoting a left turn in the 0–2 range, a right turn in the 5–7 range, and no turn otherwise.

To build our final navigation pipeline, we fuse the outputs coming from the global + local perception pipelines. PULP-Dronet’s output $\theta_{CNN} \in [-1, 1]$ is discretized with a threshold $\eta = 0.1$. We use a lookup table (LUT) to generate output pairs $(\mathbb{1}_a, \dot{\theta}_{LUT})$ for every possible combination of $(\theta_{CNN}, x_{d_{max}})$ inputs. Here, $\dot{\theta}_{LUT}$ denotes the output yaw rate, while $\mathbb{1}_a$ is a binary agreement indicator that sets the drone’s forward speed: it assumes a value of 0 when θ_{CNN} and $x_{d_{max}}$ indicate opposite steering directions, as represented by \mathbf{S} in the LUT, or it is 1 otherwise. The output yaw-rate can be either zero, indicate left and right turns at the maximum target yaw rate ($\dot{\theta}_t$ for left, $-\dot{\theta}_t$ for right), or indicate left and right turns at half of the maximum target yaw rate ($\dot{\theta}_t/2$ and $-\dot{\theta}_t/2$, respectively). The forward speed of the drone v_f , which is gated by $\mathbb{1}_a$, is adjusted in step increments as depicted in Figure 1, and depends on the average distance (d_C) measured by the four central pixels of the ToF sensor. To test the global perception pipeline in isolation, we use the CNN outputs as in [1], and for isolated testing of the local perception pipeline, we force the CNN outputs to $p_{col} = 0$ and $\theta_{CNN} = 0$.

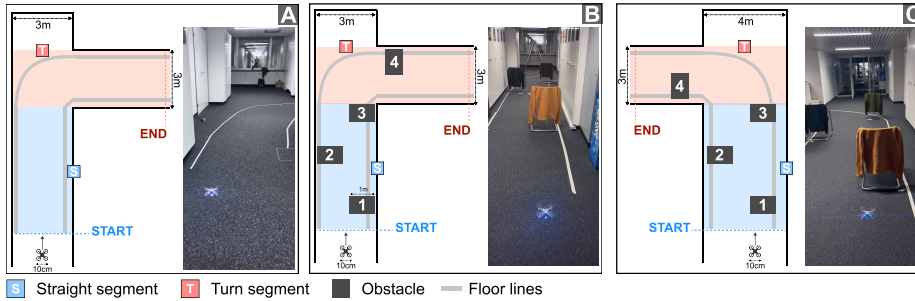


Fig. 2: The testing setups for scenario 1 (A), scenario 2 (B), and scenario 3 (C).

3 Results

We assess the navigation capabilities in an office corridor with a width of 3–4 m (Figure 2). We set up three testing scenarios, each comprising a *straight* pathway followed by a 90-degree *turn*, highlighted in Figure 2 with blue and red colors, respectively. Scenarios 1 and 2 entail a right turn (A and B), with the former obstacle-free and the latter containing four 1 m-wide obstacles. Scenario 3 (C) mirrors scenario 2, featuring a left turn and four 1 m-wide obstacles. We draw white lines on the floor, resembling the car lanes of the PULP-Dronet training dataset [1]. We assess the performance of the three perception pipelines discussed in Section 2 by conducting five flight tests per scenario, totaling 45 flights. We set the drone’s target height to 0.5 m, the target forward speed (v_t) to 1.5 m/s, and θ_t to 60 deg/s. A test is considered successful when the drone successfully flies through the corridor from **START** to **END** without collisions.

Table 1 reports the success rate of the drone for each section. Examples of the flight tests are available in the supplementary video³. In obstacle-free scenario 1, the global perception pipeline succeeds 100 % of the time, successfully recognizing the visual clues on the floor. However, this perception pipeline never succeeds in scenarios 2 and 3, colliding with the obstacles in every trial. These results confirm that PULP-Dronet v2 struggles to tackle static obstacle avoidance, as mentioned in [1]. Conversely, the local perception pipeline reliably avoids static obstacles with a 100% success rate in straight segments. Nonetheless, it consistently fails to execute turns in all scenarios, ultimately getting stuck at the end of the corridor, as the ToF can not recognize semantic elements of the environment, e.g., the floor’s line markings.

Finally, we test our fused global + local perception pipeline, which scores a 100 % success rate across both the straight and turn segments of the corridor, both when navigating in an obstacle-free corridor (scenario 1) and when tackling obstacle avoidance (scenario 2 and 3). In conclusion, our fused global + local perception pipeline captures the benefits of both the depth-based and vision-based sensory inputs: the ToF ranging measurements allow for reliable short-range static obstacle avoidance, while the PULP-Dronet understands semantic cues from its visual input, allowing the drone to follow the shape of the corridor.

³ https://youtu.be/J703fo_zIKQ

Table 1: The success rate of the three perception pipelines on three scenarios.

Perception Section	Global		Local		Global + Local	
	Straight	Turn	Straight	Turn	Straight	Turn
Scenario 1	100 %	100 %	100 %	0 %	100 %	100 %
Scenario 2	0 %	N/A	100 %	0 %	100 %	100 %
Scenario 3	0 %	N/A	100 %	0 %	100 %	100 %

4 Conclusion

We presented a pipeline for autonomous navigation on nano-UAVs that combines global and local perception. The global perception exploits the visual-based PULP-Dronet CNN to extract visual cues from the input images, while the local perception relies on an 8×8 px Time-of-Flight (ToF) sensor capturing reliable close-proximity occupancy maps. Our fused perception pipeline achieved a 100% success rate in fifteen flights, navigating through straight pathways, avoiding static obstacles, and executing a 90° turn.

Acknowledgments

We thank D. Palossi and D. Christodoulou for their contribution to this work.

References

1. V. Niculescu, L. Lamberti, F. Conti, L. Benini, and D. Palossi, "Improving autonomous nano-drones performance via automated end-to-end optimization and deployment of DNNs," *IEEE Journal on Emerging and Selected Topics in Circuits and Systems*, pp. 1–1, 2021.
2. M. J. Anderson *et al.*, "A bio-hybrid odor-guided autonomous palm-sized air vehicle," *Bioinspiration & Biomimetics*, vol. 16, no. 2, p. 026002, Dec. 2020.
3. S. Awasthi *et al.*, "UAVs for industries and supply chain management," *ArXiv*, vol. abs/2212.03346, 2022.
4. H. Müller *et al.*, "Robust and Efficient Depth-Based Obstacle Avoidance for Autonomous Miniaturized UAVs," *IEEE Transactions on Robotics*, vol. 39, no. 6, pp. 4935–4951, Dec. 2023.
5. L. Crupi *et al.*, "Sim-to-Real Vision-Depth Fusion CNNs for Robust Pose Estimation Aboard Autonomous Nano-quadcopters," in *2023 IEEE/RSJ International Conference on Intelligent Robots and Systems (IROS)*, Oct. 2023, pp. 7711–7717.
6. D. Palossi *et al.*, "An energy-efficient parallel algorithm for real-time near-optimal uav path planning," in *Proceedings of the ACM International Conference on Computing Frontiers*, ser. CF '16. New York, NY, USA: Association for Computing Machinery, 2016, p. 392–397.
7. K. McGuire *et al.*, "A comparative study of bug algorithms for robot navigation," *Robotics and Autonomous Systems*, vol. 121, p. 103261, 2019.
8. L. Lamberti *et al.*, "Bio-inspired Autonomous Exploration Policies with CNN-based Object Detection on Nano-drones," in *2023 Design, Automation & Test in Europe Conference & Exhibition (DATE)*, 2023, pp. 1–6.
9. M. Pourjabar *et al.*, "Multi-sensory anti-collision design for autonomous nano-swarm exploration," in *2023 30th IEEE International Conference on Electronics, Circuits and Systems (ICECS)*, 2023, pp. 1–5.